Effect of pulse current GMAW on the yield stress of the S460M TMCP steel welded joints

A Zavdoveev, P Zok, V Pozniakov, M Rogante, T Baudin, M Heaton, A Gaivoronskiy, S Zhdanov, P Acquier, T Solomijchuk, et al.

Effect of pulse current GMAW on the yield stress of the S460M TMCP steel welded joints

A. Zavdoveev[1], P. Zok[2], V. Pozniakov[1], M. Rogante[3], T. Baudin[4], M. Heaton[5], A. Gaivoronskiy[1], S. Zhdanov[1], P. Acquier[6], T. Solomijchuk[1], V. Kostin[1], M. Skoryk[7], I. Klochkov[1], S. Motrunich[1]

[1] Paton Electric Welding Institute of NAS, Bozhenko n. 11, 03150 Kiev, Ukraine, e-mail: avzavdoveev@gmail.com

[2] Ruhr-Universität-Bochum, Universitätsstraße 142, 44799 Bochum, Germany e-mail: peter.zok@rub.de

[3]Rogante Engineering Office, Contrada San Michele n.61, 62012 Civitanova Marche, Italy, e-mail: main@roganteengineering.it

[4]Université Paris-Saclay, CNRS, Institut de chimie moléculaire et des matériaux d'Orsay, 91405, Orsay, France, e-mail: thierry.baudin@universite-paris-saclay.fr

[5] ANT, Advanced Nano Technology, Nandor Rd, Park West business park, Dublin, e-mail: mark.heaton@antsltd.com>

[6] ADDUP FRANCE, 5 rue bleue, ZI de Ladoux, 63118 Cébazat, France, e-mail: philippeacquier@yahoo.fr

[7] G. V. Kurdyumov Institute of Metal Physics of the NAS of Ukraine; Kyiv, Ukraine, mykolaskor@gmail.com

Abstract

Thermomechanically cold processed (TMCP) steels with a high level of strength are actively used in various constructions. The high strength of the TMCP steels is acquired due to the formation of the fine-grained structure. Such steels have relatively low carbon percentage. These greatly simplify the solution of the problem of improving the quality and reliability of metal structures. At the same time this raises new questions in terms of the technology for welding such steels. In the first instance, it is conditioned by the complex behavior of the TMCP structure under the welding thermal cycle effect. The most important property of the welded joint is yield stress (YS) which characterizes the workability of the whole joint. The estimation of the YS while developing the welding technology is a valuable task for design. This current research has made a complex investigation of the modern welding technique's effect on the behavior of the yield stress formation in TMCP steel welded joints. For progressive technology development, pulse arc welding was used.

Keywords: gas metal arc welding; pulsed arc welding; heat affected zone microstructure; mechanical properties

Abbreviations

BM – base metal

COD – crack opening displacement

GMAW – gas metal arc welding

HAZ – heat affected zone

HV – Vickers hardness

PA-GMAW – pulse arc gas metal arc welding (low-frequency pulse arc welding)

PC-GMAW – pulse current gas metal arc welding

PC-GMAW F– pulse current gas metal arc welding, force mode

SEM – scanning electron microscopy

TMCP – thermomechanically cold processing (processed steel)

UTS – ultimate tensile stress

WEZ – weld zone

WTC – welding thermal cycle

YS – yield stress

1. Introduction

In recent years, the amount of welded steel constructions with higher strength abilities increased continuously. Quality requirements in many industries such as shipbuilding, civil engineering, hydropower, etc. dictate new rules for the development of welding technologies for metal structures while maintaining a high set of performance properties [1–5]. The addition of alloys in micro doses has the potential to be a key factor for higher strength[6,7]. The increase in carbon concentration offers a significant increase in strength at the same time has limitations associated with a decrease in ductility [8]. The further additional doping with elements that offer solid solution hardenings such as Mn and Si increases the strength of the metal, however, leads to a deterioration in weldability [9] due to the growth of what is known as the carbon equivalent (CE=%C+%Mn/6+(%Cr+%Mo+%V)/5+(%Cu+%Ni)/15) [2]. Microalloying with carbide and nitride-forming elements (Nb, V, Ti) is limited by the increasing cost of rolled steel.

The welding process has subjected the metal to heating that intersects critical points Ac1 Ac3, forming a heat-affected zone (HAZ) in the final welded joint [10]. Thus, the behavior of the metal under such thermal effect (welding thermal cycle) is crucial in the welded joints' mechanical properties formation, firstly due to structural transformation occurred. In this case, the mechanism of further structure evolution [4,11,12] is determined by a number of factors. During being in the temperature interval above critical points [13] Ac1, Ac3, the dispersion carbides (formed by doping elements) and carbonitrides of microalloying elements [14,15] reduce the tendency of the austenite to grow the grain size[16], either by blocking the migration of austenite grain boundaries (Zener pinning effect) [17]. In contrast to the situation for high-strength steel grades, C-Mn the concentration of the Mn is not enough for delaying grain growth of the austenite during overheating to critical points, and a high level of strength, in this case, can be reachable only for increased concentration of C to provide needed strength level.

Here in the case of microalloying, for obtaining the needed strength level, the carbon content can be reduced which thus improves their weldability (C provides the most significant input in CE), but for further increase in strength, the special techniques and approaches are required. Further increases in the yield strength of structural steels can be achieved using a special rolling method, including thermomechanical cold processing (TMCP). This requires systematic control of both temperature and degree of deformation during metal formation[12,18–20].

TMCP requires that the rolling process must be carried out in such a way that the individual stages of deformation of the steel take place at specified temperatures. There are two main effects:

- the development of fine-grained structures that improves mechanical properties and increases impact strength[21];

- the limitation or delay of recrystallization, which is achieved by the introduced microalloying elements [2,22] (Nb, Ti).

TMCP steels with a high level of strength and relatively low carbon equivalent greatly simplify the solution of the problem of improving the quality and reliability of metal structures[1,23–26]. However, this raises new questions in terms of welding technologies for such steels. Namely, the carbon equivalent alone is no longer enough for studies of the heat of TMCP steels. This is primarily due to the peculiarities of the structural state of such steels, which is not taken into account by the carbon equivalent. Technical and economic aspects arising from the ability to make products from these steels and their use in energy efficient industries, as well as their suitability for the construction of various structures, including those operating in extreme climatic conditions are of great importance for materials science. Issues related to this group of steels in order to improve the technologies used for the manufacture of metal structures from these steels by welding methods needs to be addressed. One of the promising ways to solve the problems of weldability of TMCP steels is the use of pulse-arc welding, which allows controlling the modes and thermal cycles of welding in a wide range [27–32].

Thus, weldability is determined as the formation of an equal strength joint to that of the substrate. The measurement of mechanical properties is essential, as well as structural analysis for understanding the nature of formation properties [33–36]. Since there are several parts in welded joints to be estimated, namely, weld zone (WEZ), heat-affected zone (HAZ), and base metal (BM), it puts the task of firstly mechanical properties determination for each part. The estimation of the yield stress (YS), which is the most important characteristic, meets difficulties exactly in the HAZ because of the small length of this zone. The tensile test samples can be easily cut from weld and BM, but the issue of the HAZ scale factor makes this task much more problematic. From this point of view, the indentation technique opens the way to solving this problem. In the current contribution, precise measurement is taken of the yield stress for welded joints especially in the HAZ zone, as well as a comparison with tensile tests and Vickers hardness tests made for BM

and welds. The microstructural investigation shows a good correlation with mechanical properties.

2. Experimental

The thermomechanical cold processing strengthened steel S460M [37], manufactured in accordance with EN 10025-4: 2007 is used. In all the received conditions it possesses the following mechanical properties: yield stress (YS) $R'_{p0.2}$ = 460 MPa, ultimate tensile stress (UTS) Rm = 600 MPa, δ = 25% (uniform elongation for failure), ψ = 58% (area reduction during tensile test). In case of using the TMCP steel, it is necessary to mention, that depending on the level of cold hardening effect throughout the cross-section of the material the yield strength can vary [1,26].

For the welding procedure, the G3Si1 welding wire of 1.2mm in diameter was chosen. The actual chemical compositions of the investigated steel and welding consumables measured using an optical emission spectrometer are given in Table 1.

Table 1. Chemical composition, wt. %

	C	Si	Mn	Cr	Ni	V	Nb	Al	S	P
S460M	0.15	0.23	1.3	0.09	0.019	0.01	0.05	0.025	0.013	0.017
G3Si1	0.08	0.8	1.4	0.09	0.02	0.01	-	-	0.020	0.020

The welding power source used was an inverter type ewm Phoenix Pulse 501 (company "MULTIMATRIX"), which provides a different frequency of pulses in pulse-arc welding [12]. To determine the welding and technological characteristics of the current source, a digital oscilloscope UTD2000CEX-II was used. It records the current characteristic of the power supply over a wide range. A 75mA shunt with a resistance of 150 μO was used to record the oscillograms. This allowed the registering of welding currents up to 500A, while the voltage drop across the shunt was 75 mV. The pulse current characteristics for the ewm Phoenix Pulse 501 welding source are presented in figure 1. A schematic representation of the oscillogram as well as the live one. The peaks correspond to pulse current and τ_{pulse}, and τ_{pause} is the time of the pulse and pause respectively.

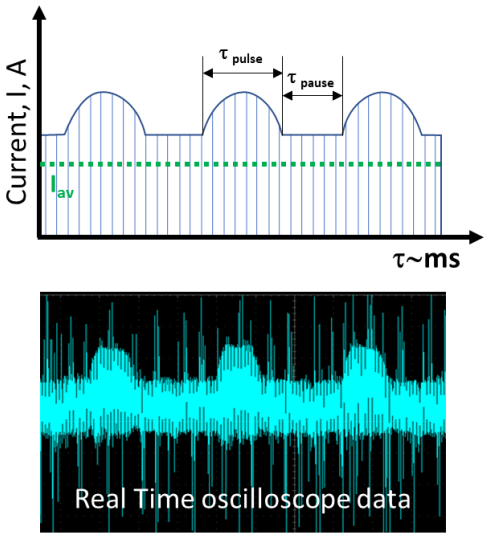

Figure 1. Pulse current characteristics.

For the basic comparative samples, the welding in shielding gas (Ar+18% CO_2) of S460M steel joints with a thickness of 16 mm and a V-shaped opening of the edges was used. Prototypes using PC-GMAW in the forced mode (PC-GMAW F) were performed for butt joints without edge machining. It should be noted that in this case, a high-quality weld formation was provided with complete welding, which is impossible in the case of using the traditional welding process. The welding modes used in the present work are presented in Table 2. From common practice, the welding current is responsible for penetration depth and welding voltage for the width of the weld [34,37]. At the same time, the welding speed is governing the heat input which is closely connected with the cooling rate of the welded joint. If the welding speed chased high, the cooling rate will be also high and this fact consequently will lead to the formation of a more hardened structure and thus a more high level of the strength of the WEZ and HAZ metal [9,13].

Table 2. Welding parameters used in this work

Welding mode	Wire diameter (mm)	Current (A)	Voltage (V)	Welding speed (mm/s)	Tip to work distance (mm)	Gas flow (l/min)	Interpass temperature (°C)
GMAW	1.2	200	16	4	12	15-20	50
PC-GMAW	1.2	220	26	4	12	15-20	50
PA-GMAW	1.2	205*	18	4	12	15-20	50
PC-GMAW F	1.2	320	28	5	12	15-20	-

*Here: $I_{av} = \frac{I_{pulse}t_{pulse} + I_{pause}t_{pause}}{t_{pulse} + t_{pause}}$, where I_{pulse} = 220 A, I_{pause} = 0.8*I_{pulse} t_{pulse} = 0.5s, and t_{pause} = 0.25s are the pulse duration and pause, respectively.

The common welding parameter i.e wire diameter, tip to work distance (is equal to 10 times wire diameter), interpass temperature, and welding speed are chosen based on practice and previous experiments [30,37].

In order to study the influence of the welding modes on welding thermal cycles (WTC), appropriate experiments were performed. Steel plates, 10 mm thick were used to register the WTC, into which chromel-alumel thermocouples were drilled to a depth of 7.5–8 mm. This value of the drilling depth is based on previous studies [25] and is due to the need to register the WTC in the area of the HAZ.

The pointwise mechanical characterization was carried out through minor destructive indentation techniques, 3D measurements of these indents and inverse analyses by finite-element material models. This method is called "Eindruckverfahren" or Imprint-Testing [38] and provides the following values (Figure 2.):

- $R^I_{p0,2}$ comparative yield strength (Imprint) strength
- R^I_m comparative ultimate tensile strength (Imprint)
- D is the ductility value based on plastic elongation (Note - this value is not directly comparable to the strain from the tensile test, but there is a linear trend [38])

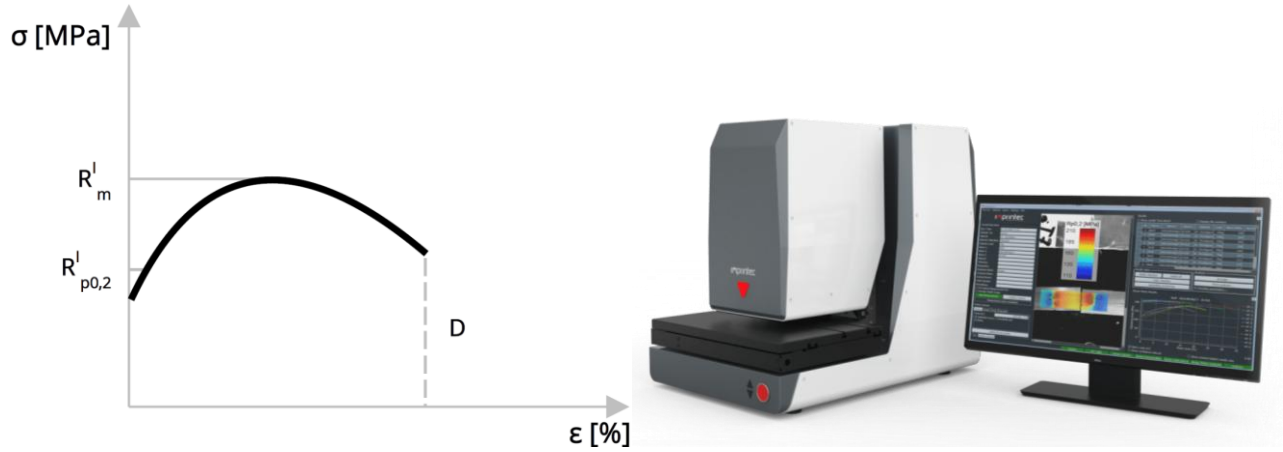

a) b)

Figure 2. The plastic flow schematic curve determined with indentation technique called ”Eindruckverfahren” (Imprintec) (a); The testing tool in general view (b)

The Rockwell cone indentation measurements of the investigated samples were made with the following mesh consisting of 3 lines equidistant from each other on 0.5 mm and 20 points per line (the distance between points is 0.5mm).

Standard cylindrical tension samples were made of welded joints for mechanical testing of the weld metal for comparison purposes. Three samples for each measurement with a 6 mm diameter for their working parts were mechanically manufactured (type II following ISO 6892:1998). The tests were carried out at an ambient temperature. The tests were carried out at an ambient temperature.

Metallographic studies were performed using a scanning electron microscope on the Miga C LMU (Tescan). The samples for the metallographic studies were prepared according to standard methods using diamond pastes of different dispersion. The detection of microstructure was performed by chemical etching in 4% alcohol solution with nitric acid. The Vickers microhardness of the individual structural components and the integral hardness of the metal was measured on a hardness tester M-400 company "LECO" at a load of 100 g (HV).

The ability of the metal to resist brittle fracture was determined using approaches to fracture mechanics. The values of the criteria K_{1C} and δ_C defined below were determined by the standard methods and formulas given in [32].

To determine the values of the critical stress intensity factor K_{1C} and the critical crack opening δ_C, samples of rectangular cross section 10x20x90 mm^3 with a notch length of 7 mm and a fatigue crack of 3 mm length were used. These samples were tested for three-point bending at room temperature.

3. Results and discussion

3.1. Structure and properties of the base metal

Owing to TMCP with controlled cooling in the temperature range 900-700°C in ferrous S460M ferritic-pearlitic steel, a striped structure with a grain size of about 10 μ is formed with a hardness of 195 HV (Figure 3).

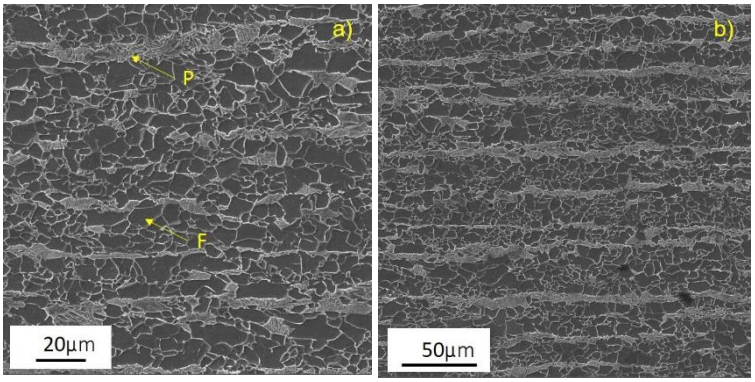

Figure 3. Microstructure of the base metal in as-received condition (P: pearlite, F: ferrite) – (a) high magnification (b) - low magnification

3.2. Mechanical properties

3.2.1. Microhardness analysis

The study of the hardness (Figure 4) of welded joints revealed that when PC-GMAW F is used, the WEZ metal hardness is 15-20% lower than the hardness of the weld metal made by standard PC-GMAW and PA-GMAW respectively. When for GMAW mode they are almost equal value. This is due to the peculiarities of the structure formation caused by the welding thermal cycle (WTC) which will be considered below. In the HAZ metal, the hardness values of PC-GMAW F are also lower than in standard PC-GMAW. This fact is an additional advantage of PC-GMAW F, as a uniform distribution of mechanical properties will be formed in the welded joint. It should be noted that, with PC-GMAW F, the hardness in the HAZ decreases to the level of the base metal more slowly.

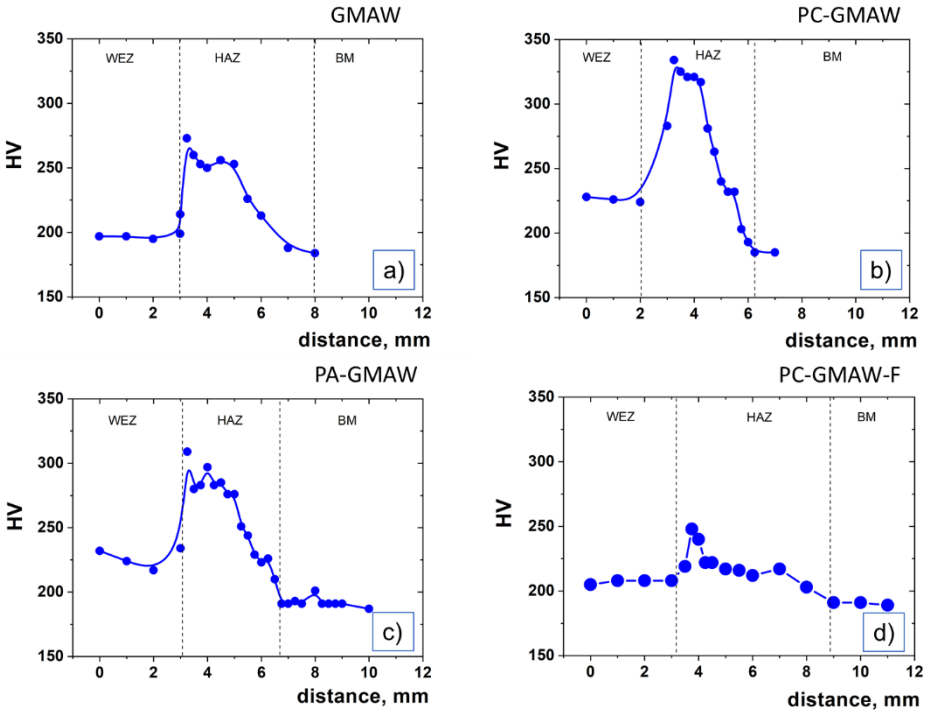

Figure 4 Hardness of S460M steel welded joints: GMAW (a), PC-GMAW (b), PA-GMAW (c), PC-GMAW -F (d)

3.2.2. Indentation analysis

In the extended analyses with the indentation technique “Eindruckverfahren” the strength levels according to the YS and UTS become evident. The comparison between the welded joint with forced PC-GMAW F and the three other joints (GMAW, PC-GMAW, PA-GMAW) revealed that the forced PC-GMAW F joint has a quiet homogenous distribution of the YS and UTS over the WEZ, HAZ and BM zones. The other welded joints have a more heterogeneous distribution, or rather a distinct strength-gradient over the WEZ, HAT and BM (Figure 5 and 6):

- a) GMAW: distribution of YS is approx. 140 MPa and UTS is approx. 120 MPa
- b) PC-GMAW: distribution of YS is approx. 367 MPa and UTS is approx. 340 MPa
- c) PA-GMAW: distribution of YS is approx. 307 MPa and UTS is approx. 241 MPa
- d) PC-GMAW-F: distribution of YS is approx. 70 MPa and UTS is approx. equal to 100 MPa

Loading curves for measuring mesh are presented in figure 5, where it can be observed a clear tendency for homogeneous distribution for PC-GMAW-F mode. This effect is conditioned by structure formation and will be considered below. From this point of view, there is a good correlation with hardness measurements.

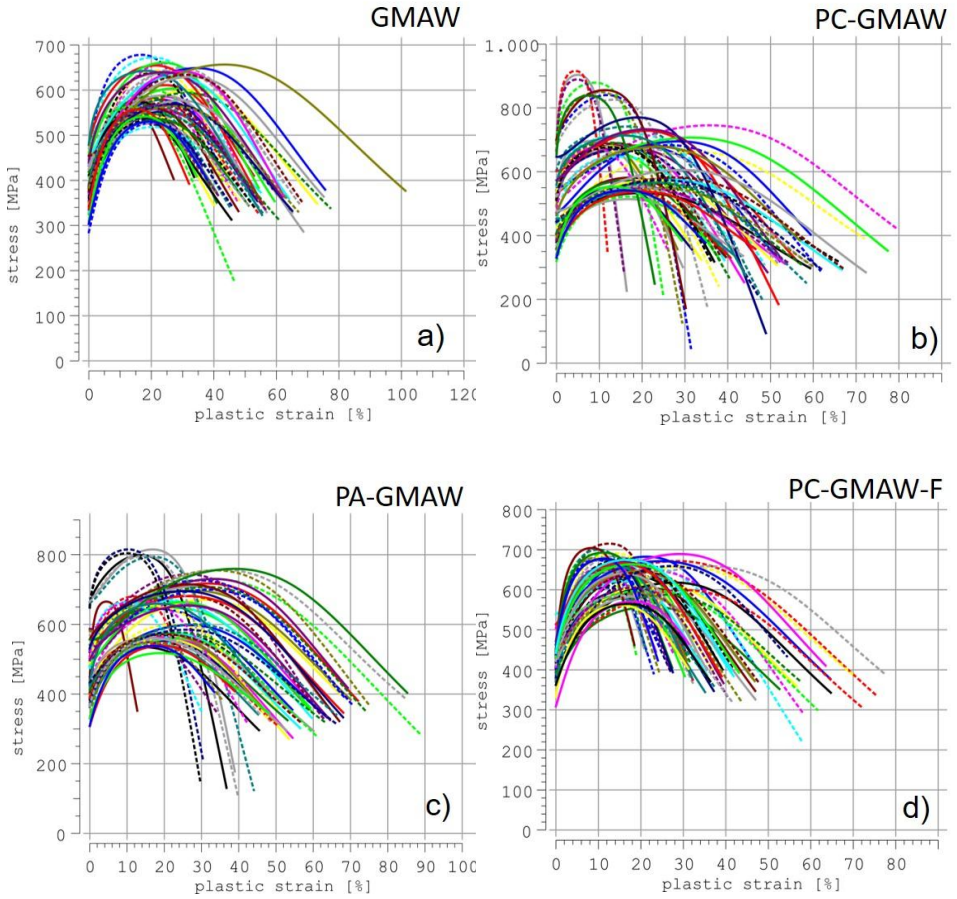

Figure 5. Loading curves for welded joints of S460M steel made by different welding modes: GMAW (a), PC-GMAW (b), PA-GMAW (c), PC-GMAW -F (d). (Number of curves correspond to mesh nodes)

As well as for loading curves and calculated data of yield stress and ultimate tensile stress are also in good correlation (figure 6). For the determination of the UTS, a strong correlation exists with microhardness. Similar behavior of the yield stress on a lower strength level is observed. The value of the error is conditioned by the number of measurements per point on the graph. Here, averaged values were determined from 3 lines to get one point. In the HAZ due to the V type edge development the calculation can take part in several zones.

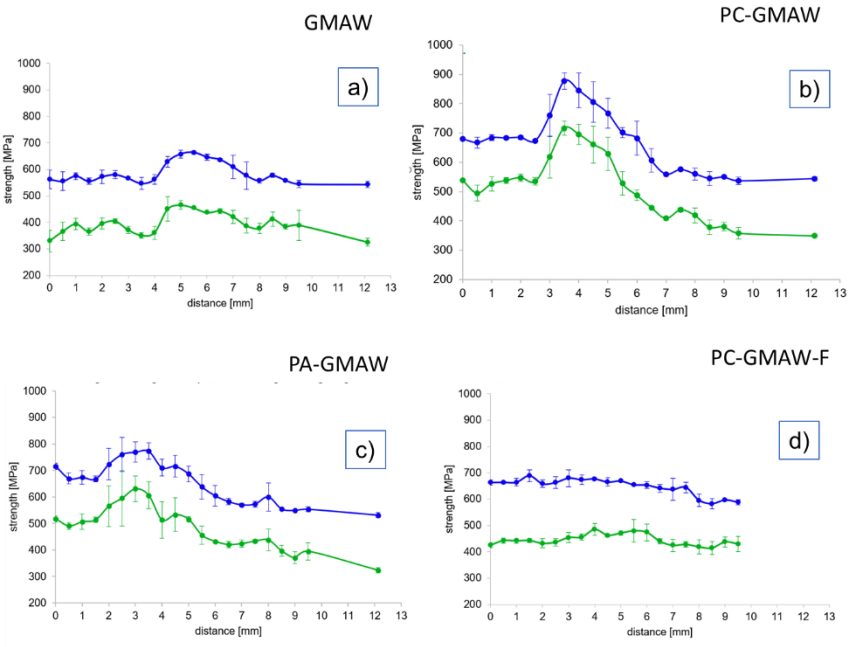

Figure 6. The distribution of the YS (green) and UTS (blue) for welded joints of S460M steel made by different welding modes : GMAW (a), PC-GMAW (b), PA-GMAW (c), PC-GMAW -F (d).

For a better visualization, the R'p0.2 and Rm maps for welded joints are built in Figure 7 and Figure 8, respectively. It is clearly seen that PC-GMAW and PA-GMAW provide more high level of stress (R'p0.2, Rm). The most favorable distribution of the stress (R'p0.2, Rm) is provided by PC-GMAW F mode, because of dispersion of the yield stress and ultimate tensile stress are minimal in comparison with other welding techniques.

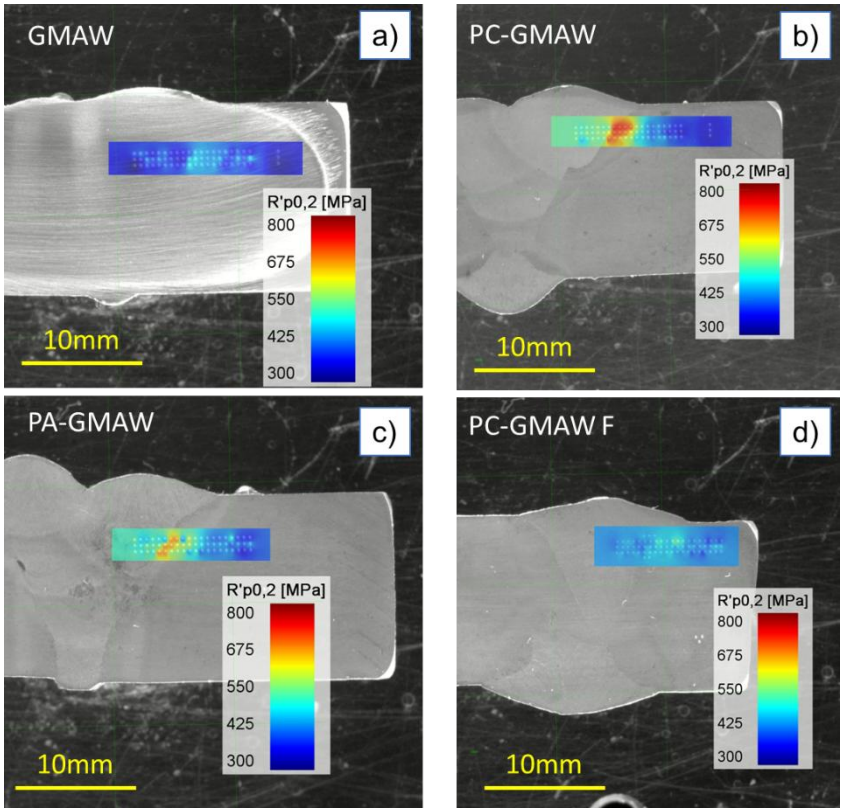

Figure 7. The YS maps for welded joints of S460M steel made by different welding modes : GMAW (a), PC-GMAW (b), PA-GMAW (c), PC-GMAW -F (d).

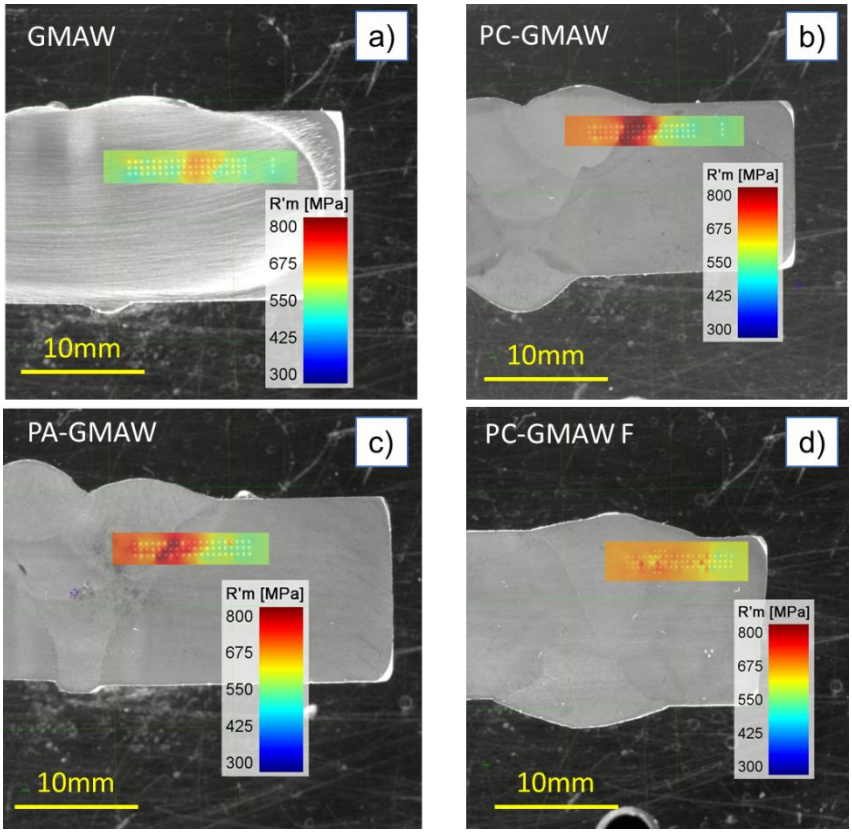

Figure 8. The UTS maps for welded joints of S460M steel made by different welding modes : GMAW (a), PC-GMAW (b), PA-GMAW (c), PC-GMAW -F (d).

From the given YS and UTS maps (Figure 7 and 8) the distribution of strength values is shown pointwise. Especially the HAZ from PC-GMAW and PA-GMAW becomes evident for its increased values. The pointwise determined YS and UTS confirm and expand the expression of heterogeneous or homogeneous mechanical properties in the different welding joints.

3.2.3 Tensile test analysis

For comparison with indentation, standard tensile tests were performed and the slight difference in yield stress (measured by tensile test) is explained by the scale factor of the tested samples. From the data given in table 3 it is seen that under the conditions of pulse-arc welding that higher values of the strength of the weld metal are achieved in comparison with the base metal. Plasticity remains at a fairly high level. The values of the strength of the weld metal are in good agreement with the hardness values for the area of the weld metal, namely do not exceed the values of the base metal by more than 20%. When using PC-GMAW F, given that the hardness of the HAZ metal is not more than 20-25% of the base metal, this ensures the uniformity of the welded joint.

Table 3. Mechanical properties of the weld metal of S460M steel.

	Welding technique	YS, MPa	UTS, MPa	δ	ψ
Weld metal (WEZ)	PC-GMAW	570	667	24	68
	PC-GMAW F	590	675	23	55
	PA-GMAW	590	680	26	70
	GMAW	477	586	28	73
BM		452	581	26	60

The behavior of mechanical properties described above is explained by microstructural evolution in dependence on the welding mode and presented below.

3.2.3. Microstructure analysis

The explanation of the mechanical properties evolution during different welding modes used in the present work, namely GMAW, PC-GMAW, PA-GMAW, and PC-GMAW-F gave by microstructural analysis. The main consideration is focused on the WEZ

and HAZ metal. The following microstructural features can be observed. The ferrite structure of various modifications (polygonal, large-needle) in the WEZ metal is formed during GMAW. The characteristic size of the polyhedral ferrite in length is more than 100 μm with coarse-grained needle-like ferrite (Figure 9 a).

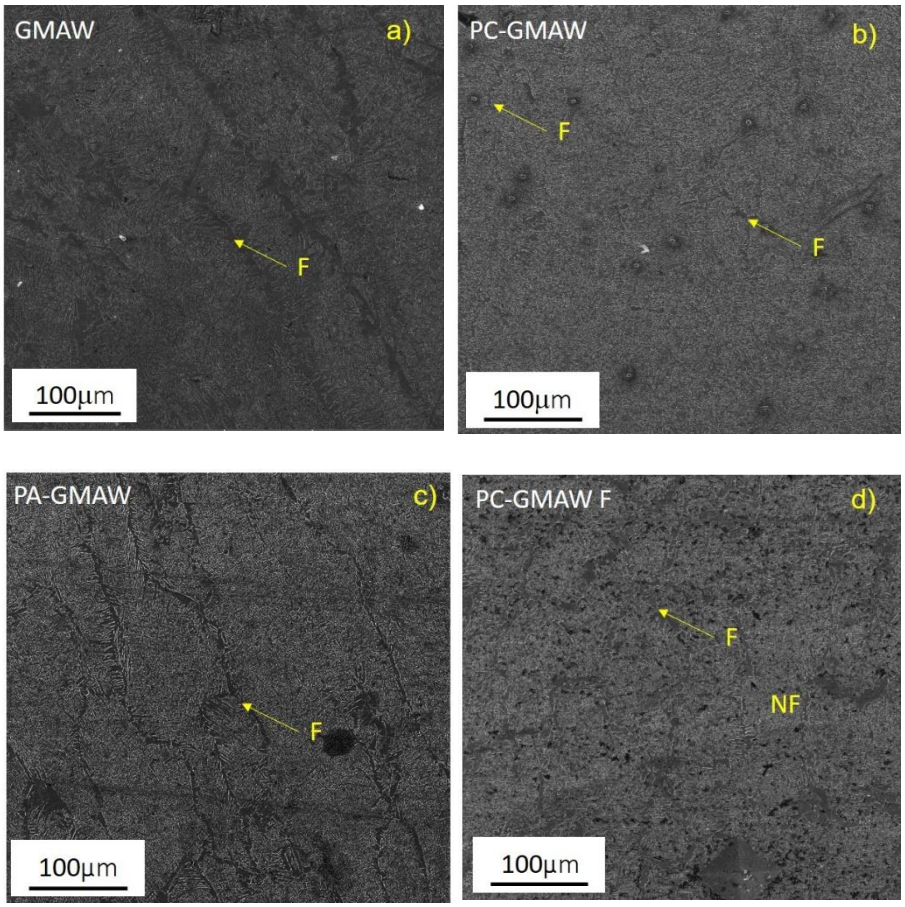

Figure 9. The microstructure of the WEZ metal for S460M steel joints : GMAW (a), PC-GMAW (b), PA-GMAW (c), PC-GMAW -F (d).

Such structure formation is conditioned firstly by the cooling rate provided by GMAW mode. In the case of the PC-GMAW owing to changes in cooling rate (WTC), the microstructure of the WEZ metal consists of refined bainite (1…3 μm) and a reduced amount of polyhedral ferrite (marked by arrow) and secretions of polygonal ferrite (3-10 μm), located along the boundaries of the primary austenitic grains (Figure 9 b). Further welding mode (PA-GMAW) is characterized by changed WTC and leads to the formation of the somewhat finer bainite and narrower polygonal ferrite (WEZ metal) in comparison with GMAW mode and slightly larger in comparison with PC-GMAW mode (Figure 9 c). The most significant changes are observed in the case of the PC-GMAW F mode, namely the microstructure of the WEZ metal differs significantly from the other welding modes. The needle-like ferrite (NF) with large plates is observed, and the allocation of polygonal ferrite became wider and their share increased (Figure 9 d). For the HAZ metal (Figure 10)

the microstructure of the upper and lower bainite for GMAW and PA-GMAW mode, a bainite structure with a small proportion (up to 3… 5%) of the martensite for PC-GMAW mode, and finally, mainly needle ferrite with an ordered second phase for PC-GMAW F mode are observed.

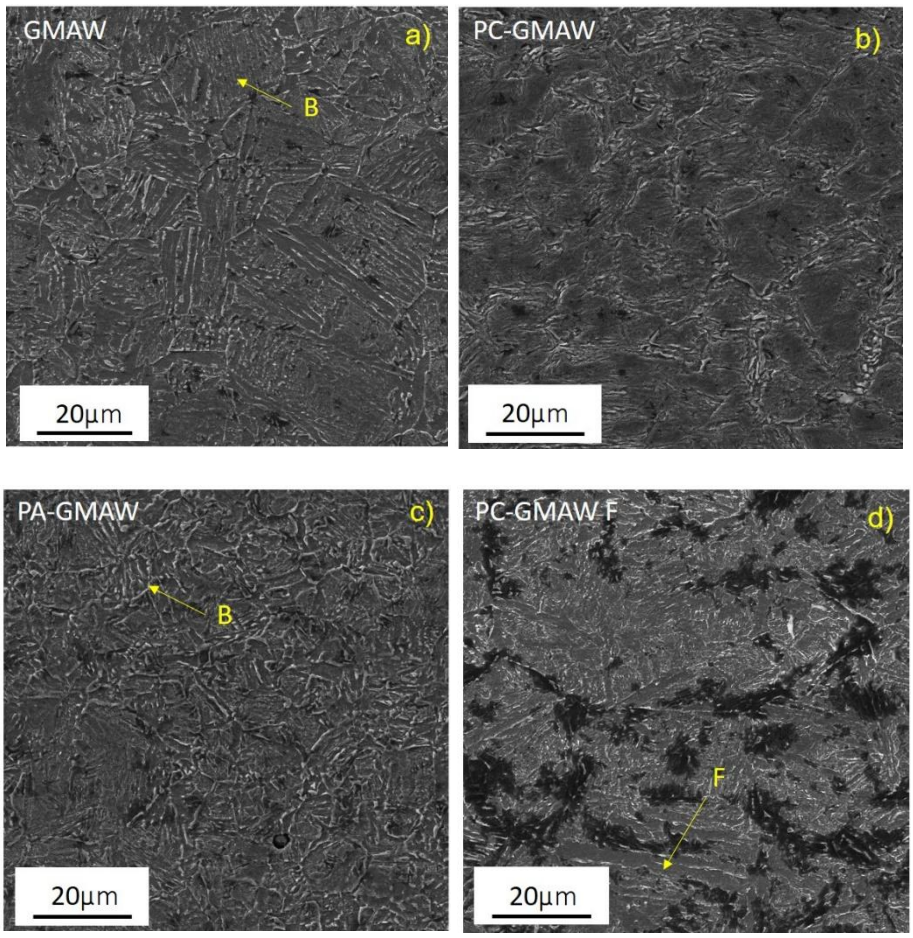

Figure 10. The microstructure of the HAZ metal for S460M steel joints : GMAW (a), PC-GMAW (b), PA-GMAW (c), PC-GMAW -F (d).

Such differences are due to the peculiarities of the WTC during pulse-arc welding (Figure 11). Arc welding is characterized by physical and metallurgical processes so that one understands the number of complex objects that occurred in the molten metal [39], and the metal of the HAZ under the effect of the welding thermal cycle (WTC), so the main factor affecting it is the WTC. The WTC is characterized by parameters like maximum temperature, heating and cooling rate, time above the set temperatures and in the temperature range. It is possible to control the WTC by changing the modes of the pulse

GMAW, namely the main components of current, welding voltage, frequency and duty cycle, and welding speed.

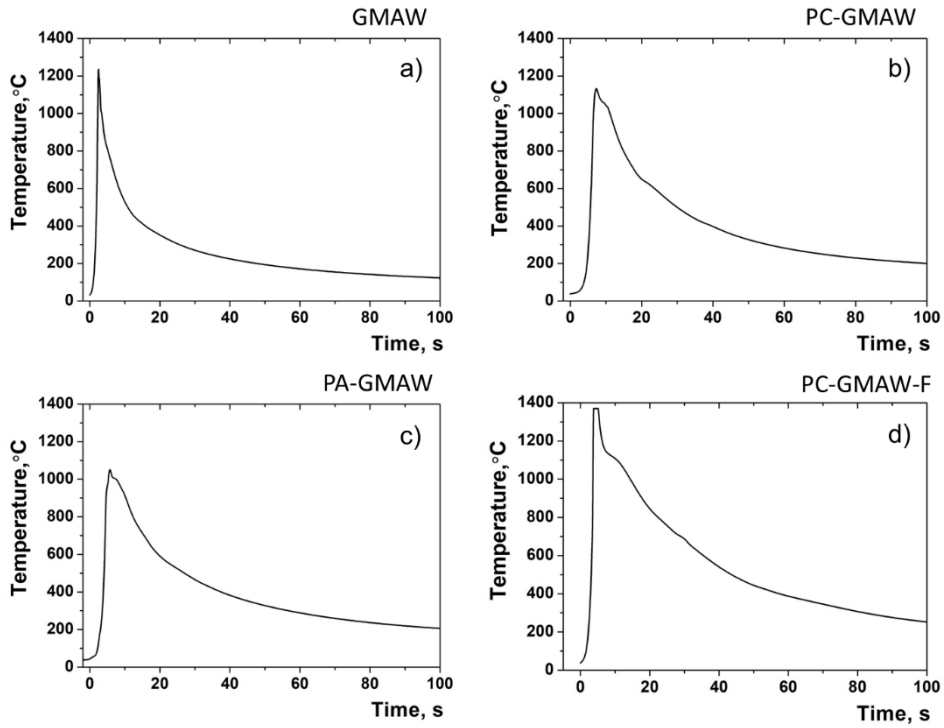

Figure 11. Thermal welding cycles for different welding modes : GMAW (a), PC-GMAW (b), PA-GMAW (c), PC-GMAW -F (d)

Therefore, it is advisable to consider the features of the WTC. The given data testify that it qualitatively differs from WTC characterized to GMAW. It has the following features: in the case of PC-GMAW and PC-GMAW-F, the rate of increase in the temperature is greater than in the case of GMAW; in the high-temperature range from 1350 ^{o}C to 1000 ^{o}C, the cooling of the metal is faster, and in the temperature range less than 1000 °C - slower. The peculiarities of the WTC flow during PC-GMAW and PC-GMAW-F, allowed to establish that the cooling rate of the metal in the HAZ areas heated to temperatures of 1000 °C and more is higher than in stationary arc welding. In the HAZ metal, where the metal is heated to temperatures below 1000 °C, the cooling rate of the metal is lower than at GMAW. This promotes the flow of diffusion processes during structural transformations. Similar patterns are observed in PA-GMAW (Figure 11 c), namely, the cooling rate of HAZ metal in the temperature range of 600-500 ^{o}C is less than in standard GMAW.

The WTC plays a key role in the hardening of the weld metal, as it affects the refinement of structural components. During pulsed arc welding there is an interruption in an arc which causes a thermal "blow" that leads to increasing the number of the centers of

crystallization. As a result, the structure is refined and the strength characteristics are increased.

3.2.4. Fracture toughness

To assess the sensitivity of metal parts of welded joints to the stress concentration under conditions of flat deformation under static load, a force criterion is used - the critical stress intensity factor K_{1C}. As the values of K_{1C} increase, the sensitivity of the metal to the stress concentration decreases. Deformation fracture criteria are used to determine the crack resistance of fracture materials, which are accompanied by significant plastic deformations in the area near the top of the crack and precedes its spread. This criterion is called the critical opening of the crack tip - δ_C. If the shore opening is greater than δ_C, then the adhesion stress is zero.

The values of the criteria K_{1C} and δ_C were determined by standard methods. To determine the values of the critical stress intensity factor K_{1C} the next formula is used [32]:

$$K_{1C} = \frac{P \cdot L \cdot Y}{t \cdot \sqrt{b^3}} \qquad (1),$$

where: P is the critical load at which the sample collapses; L is the distance between the supports; t is the thickness of the sample; b is the width of the sample; Y is the shape factor of the sample.

The critical opening of the crack (crack opening displacement) δ_c is determined by the formula:

$$\delta_C = \frac{4 \cdot {K_{1C}}^2}{\pi \cdot YS \cdot E} \qquad (2),$$

where: YS – yield stress (is determined by indentation), E is the Young's modulus which is equal to 200 GPa for low carbon steel [4].

It is used to estimate the resistance of the metal to brittle fracture under conditions of large plastic deformation, when the crack at its apex reaches the critical size of δ_C and begins to propagate rapidly, using the energy released during its further growth. The indicators of resistance to brittle fracture of HAZ metal of welded joints made of standard and forced pulse-arc welding are at a high level, due to the peculiarities of the formation of the structure (Figure 12). As crack opening displacement (COD, δ_c) can give additional information about ductility and the ability of the metal to resist crack propagation, and based on the indentation results it becomes possible to estimate (using eq.2) the COD.

Here it is seen that despite K1C slight difference (within 5 %) the value of the COD has more significant dispersion up to 75 % (Figure 12 b). From the data it is clear that from point of view of plasticity mechanics the PC-GMAW – F provides the best characteristics.

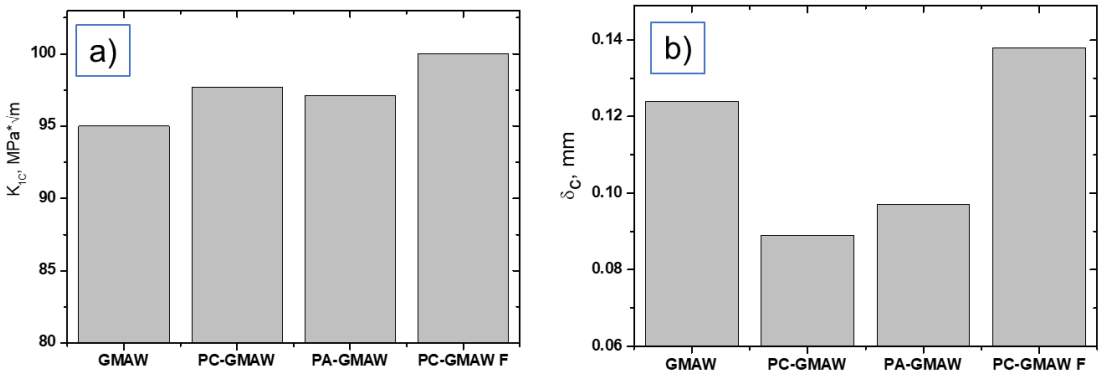

Figure 12 Fracture toughness and crack opening displacement

(a) - K_{1C} and (b) - COD

The pulse-arc welding allows to effectively regulate the structure in the welded joints of high-strength TMCP steels. Under conditions of approximately the same running energies, the effective welding current of the pulse-arc process is 25% higher than when welding with GMAW. This allows the depth of penetration to be increased. Features of the pulse change of the welding current significantly change the nature of the WTC and as a consequence the structure of the thermal zone. The formation of a mixed structure in HAZ allows high strength and resistance to brittle fracture to be obtained. The use of the PC-GMAW F gives the opportunity to make quality welded joints with uniform distribution of the yield stress, which is explained by the features of structural formation governed by WTC. These above-described results allow the following conclusions to be made:

4. Conclusions

Due to the change of WTC (increases in cooling rate in the temperature range > 1000^{o}C), the analysis of experimental data has shown that usage of PC-GMAW leads to a fine-grained structure in the weld in comparison with GMAW, and metal hardening structures in the HAZ. The cooling rate of HAZ metal in the temperature range of 600-500^{o}C is reduced by almost 1.5 times, which reduced the width of the HAZ by 40%. As a

result of tests, it was found that the metal of the weld and the HAZ of the welded joints of S460M steel, made by pulse-arc welding, have a sufficiently high resistance to brittle fracture, and 20% higher strength.

Studies of the influence of standard and forced pulse-arc welding on the structure and mechanical properties of TMCP and treated steel S460M allowed to establish the following advantages of the latter:

- in comparison with standard pulse-arc welding, the forced PC-GMAW allows carrying out welding without the development of edges when receiving high-quality welded joints

- 30% lower values of microhardness, as well as yield stress, in the HAZ of the welded joint in comparison with the standard GMAW due to the peculiarities of the thermal cycle of welding.

- 15% lower values of microhardness of the weld metal compared to PC-GMAW and PA-GMAW and close to the values of the base metal, which is provided by the formation of a favorable microstructure

- higher homogenous distribution of YS and UTS over the WEZ and HAZ close to the strength level of BM

- high level of resistance to brittle fracture of the welded joints, as well as crack opening displacement calculated based on the yield stress data after indentation.

These features of forced pulse-arc welding ensure high mechanical properties of welded joints of TMCP hardened steel S460M, which is the main task for this class of steel. It is demonstrated that the possibility of conducting PC-GMAW F without the development of edges, in addition, can increase the productivity of the process by 40%.

Acknowledgments

This work was supported by the National Academy of Sciences of Ukraine [grant number 0117U001666]. The authors are grateful to Dr A. Shishkevich for his help in the experiments.

Statements and Declarations

Funding

This work was supported by the National Academy of Sciences of Ukraine [grant number 0117U001666].

Conflict of interest: Anatoliy Zavdoveev, Peter Zok, Valeriy Pozniakov, Massimo Rogante, Thierry Baudin, Mark Heaton, Alex Gaivoronskiy, Sergiy Zhdanov, Philippe Acquier, Tatiana Solomijchuk, Valeriy Kostin, Mykola Skoryk, Ilya Klochkov, Sviatoslav Motrunich declare that they have no conflict of interest.

Author Contributions

Anatoliy Zavdoveev, Peter Zok, Thierry Baudin and Philippe Aquier Conceptualization, Methodology **Anatoliy Zavdoveev, Valeriy Poznyakov, Alex Gajvoronskiy** Supervision **Ilya Klochkov, Sviatoslav Motrunich, Massimo Rogante, Tatiana Solomijchuk, Valeriy Kostin, Sergiy Zhdanov, Mykola Skoryk and Mark Heaton** Data curation, Writing- Original draft preparation. All authors discussed the results and commented on the manuscript.

Reference

[1] C.H. Lee, H.S. Shin, K.T. Park, Evaluation of high strength TMCP steel weld for use in cold regions, J. Constr. Steel Res. (2012). https://doi.org/10.1016/j.jcsr.2012.02.012.

[2] S.F. Medina, M. Gómez, P.P. Gómez, Effects of v and Nb on static recrystallisation of austenite and precipitate size in microalloyed steels, J. Mater. Sci. (2010). https://doi.org/10.1007/s10853-010-4616-z.

[3] C. Fossaert, G. Rees, T. Maurickx, H.K.D.H. Bhadeshia, The effect of niobium on the hardenability of microalloyed austenite, Metall. Mater. Trans. A. (1995). https://doi.org/10.1007/BF02669791.

[4] A. Zavdoveev, V. Poznyakov, T. Baudin, M. Rogante, H.S. Kim, M. Heaton, Y. Demchenko, V. Zhukov, M. Skoryk, Effect of heat treatment on the mechanical properties and microstructure of HSLA steels processed by various technologies, Mater. Today Commun. 28 (2021) 102598. https://doi.org/https://doi.org/10.1016/j.mtcomm.2021.102598.

[5] A.V. Zavdoveev, S.L. Zhdanov, A.V. Maksimenko, V.D. Poznyakov, Influence of thermal cycle of welding on structure and mechanical properties of haz metal in high-strength steel produced by controlled rolling, Pat. Weld. J. (2018).

https://doi.org/10.15407/tpwj2018.10.02.

[6] J. Moon, C.-H. Lee, H.-H. Jo, S.-D. Kim, H.-U. Hong, J.-H. Chung, B.H. Lee, Microstructure and High-Temperature Strength in the Weld Coarse-Grained Heat-Affected Zone of Fire-Resistant Steels and the Effects of Mo and Nb Additions, Met. Mater. Int. 28 (2022) 966–974. https://doi.org/10.1007/s12540-020-00947-8.

[7] T.V.S. Rajan, C.P. Sharma, A. Sharma, Heat treatment: principles and techniques, PHI Learning Pvt. Ltd., 2011.

[8] J.-H. Sim, T.-Y. Kim, J.-Y. Kim, C.-W. Kim, J.-H. Chung, J. Moon, C.-H. Lee, H.-U. Hong, On the Strengthening Effects Affecting Tensile and Low Cycle Fatigue Properties of Low-Alloyed Seismic/Fire-Resistant Structural Steels, Met. Mater. Int. 28 (2022) 337–345. https://doi.org/10.1007/s12540-020-00870-y.

[9] G. Park, S. Jeong, C. Lee, Fusion Weldabilities of Advanced High Manganese Steels: A Review, Met. Mater. Int. 27 (2021) 2046–2058. https://doi.org/10.1007/s12540-020-00706-9.

[10] G. Janardhan, K. Kishore, G. Mukhopadhyay, K. Dutta, Fatigue Properties of Resistance Spot Welded Dissimilar Interstitial-Free and High Strength Micro-Alloyed Steel Sheets, Met. Mater. Int. 27 (2021) 3432–3448. https://doi.org/10.1007/s12540-020-00678-w.

[11] M. Liu, J. Wang, Q. Zhang, H. Hu, G. Xu, Optimized Properties of a Quenching and Partitioning Steel by Quenching at Fine Martensite Start Temperature, Met. Mater. Int. 27 (2021) 2473–2480. https://doi.org/10.1007/s12540-020-00726-5.

[12] Z. Nasiri, S. Ghaemifar, M. Naghizadeh, H. Mirzadeh, Thermal Mechanisms of Grain Refinement in Steels: A Review, Met. Mater. Int. 27 (2021) 2078–2094. https://doi.org/10.1007/s12540-020-00700-1.

[13] M. Shome, O.P. Gupta, O.N. Mohanty, Effect of simulated thermal cycles on the microstructure of the heat-affected zone in HSLA-80 and HSLA-100 steel plates, Metall. Mater. Trans. A. 35 (2004) 985–996.

[14] T. Sakthivel, C.R. Das, K. Laha, G. Sasikala, Creep Properties of Intercritical Heat Treated Boron Added Modified 9Cr–1Mo Steel, Met. Mater. Int. 27 (2021) 328–336. https://doi.org/10.1007/s12540-019-00377-1.

[15] Z. Li, P. La, J. Sheng, Y. Shi, X. Zhou, Q. Meng, Outstanding Synergy of Superior Strength and Ductility in Heterogeneous Structural 1045 Carbon Steel, Met. Mater.

Int. 27 (2021) 2562–2574. https://doi.org/10.1007/s12540-020-00662-4.

[16] T.-Y. Kim, T.-W. Na, H.-S. Shim, Y.-K. Ahn, Y.-K. Jeong, H.N. Han, N.-M. Hwang, Misorientation Characteristics at the Growth Front of Abnormally-Growing Goss Grains in Fe–3%Si Steel, Met. Mater. Int. 27 (2021) 5114–5120. https://doi.org/10.1007/s12540-020-00794-7.

[17] J. Moon, C. Lee, Pinning efficiency of austenite grain boundary by a cubic shaped TiN particle in hot rolled HSLA steel, Mater. Charact. 73 (2012) 31–36.

[18] K. Chadha, C. Aranas, M. Jahazi, Effect of Double Hit Hot Deformation on the Evolution of Dynamically Transformed Ferrite, Met. Mater. Int. 27 (2021) 4307–4321. https://doi.org/10.1007/s12540-020-00855-x.

[19] S. Kumar, A. Karmakar, S.K. Nath, Comparative Assessment on the Hot Deformation Behaviour of 9Cr–1Mo Steel with 1Cr–1Mo Steel, Met. Mater. Int. 27 (2021) 3875–3890. https://doi.org/10.1007/s12540-020-00826-2.

[20] B. Jiang, X. Hu, L. Zhou, H. Wang, Y. Liu, F. Gou, Effect of Transformation Temperature on the Ferrite–Bainite Microstructures, Mechanical Properties and the Deformation Behavior in a Hot-Rolled Dual Phase Steel, Met. Mater. Int. 27 (2021) 319–327. https://doi.org/10.1007/s12540-019-00371-7.

[21] U. Mayo, N. Isasti, J.M. Rodriguez-Ibabe, P. Uranga, On the characterization procedure to quantify the contribution of microstructure on mechanical properties in intercritically deformed low carbon HSLA steels, Mater. Sci. Eng. A. 792 (2020) 139800. https://doi.org/https://doi.org/10.1016/j.msea.2020.139800.

[22] G. Larzabal, N. Isasti, J. Rodriguez-Ibabe, P. Uranga, Effect of Microstructure on Post-Rolling Induction Treatment in a Low C Ti-Mo Microalloyed Steel, Metals (Basel). (2018). https://doi.org/10.3390/met8090694.

[23] B. De Meester, The weldability of modern structural TMCP steels, ISIJ Int. 37 (1997) 537–551. https://doi.org/10.2355/isijinternational.37.537.

[24] S. Lee, B.C. Kim, D. Kwon, Correlation of microstructure and fracture properties in weld heat- affected zones of thermomechanically controlled processed steels, Metall. Trans. A. (1992). https://doi.org/10.1007/BF02651759.

[25] A. Zavdoveev, V. Poznyakov, T. Baudin, M. Heaton, H.S. Kim, P. Acquier, M. Skory, M. Rogante, A. Denisenko, Welding Thermal Cycle Impact on the Microstructure and Mechanical Properties of Thermo–Mechanical Control Process Steels, Steel Res.

Int. (2021). https://doi.org/10.1002/srin.202000645.

[26] D. Porter, A. Laukkanen, P. Nevasmaa, K. Rahka, K. Wallin, Performance of TMCP steel with respect to mechanical properties after cold forming and post-forming heat treatment, Int. J. Press. Vessel. Pip. (2004). https://doi.org/10.1016/j.ijpvp.2004.07.006.

[27] J.C. Needham, Material transfer characteristics with pulsed current, Brit. Weld. J. 12 (1965).

[28] P.K. Palani, N. Murugan, Selection of parameters of pulsed current gas metal arc welding, J. Mater. Process. Technol. 172 (2006) 1–10. https://doi.org/https://doi.org/10.1016/j.jmatprotec.2005.07.013.

[29] H. Tong, T. Ueyama, S. Harada, M. Ushio, Quality and productivity improvement in aluminium alloy thin sheet welding using alternating current pulsed metal inert gas welding system, Sci. Technol. Weld. Join. 6 (2001) 203–208. https://doi.org/10.1179/136217101101538776.

[30] A. Zavdoveev, M. Rogante, V. Poznyakov, M. Heaton, P. Acquier, H.S. Kim, T. Baudin, V. Kostin, Development of the PC-GMAW welding technology for TMCP steel in accordance with welding thermal cycle, welding technique, structure, and properties of welded joints, Reports Mech. Eng. 1 (2020) 26–33. https://www.frontpres.rabek.org/index.php/asd/article/view/3.

[31] S. Rajasekaran, Weld Bead Characteristics in Pulsed GMA Welding of AI-Mg Alloys, Weld. J. 78 (1999) 12.

[32] A. V Zavdoveev, V.D. Poznyakov, M. Rogante, S.L. Zhdanov, V.A. Kostin, T.G. Solomiychuk, Features of structure formation and properties of joints of s460m steel made by pulsed-arc welding, Pat. Weld. J. (2020) 9–13. https://doi.org/https://doi.org/10.37434/tpwj2020.06.02.

[33] A. V. Nazarov, E. V. Yakushev, I.P. Shabalov, Y.D. Morozov, T.S. Kireeva, Comparison of weldability of high-strength pipe steels microalloyed with niobium, niobium and vanadium, Metallurgist. (2014). https://doi.org/10.1007/s11015-014-9821-6.

[34] J. Górka, Weldability of Thermomechanically Treated Steels Having a High Yield Point, Arch. Metall. Mater. (2015). https://doi.org/10.1515/amm-2015-0076.

[35] H. Nam, C. Park, C. Kim, H. Kim, N. Kang, Effect of post weld heat treatment on

weldability of high entropy alloy welds, Sci. Technol. Weld. Join. 23 (2018) 420–427. https://doi.org/10.1080/13621718.2017.1405564.

[36] J. Górka, Assessment of Steel Subjected to the Thermomechanical Control Process with Respect to Weldability, Metals (Basel). (2018). https://doi.org/10.3390/met8030169.

[37] A.V. Zavdoveev, S.L. Zhdanov, A.A. Maksimenko, T.G. Solomijchuk, V.D. Poznyakov, Weldability of high-strength microalloyed steel S460M, Pat. Weld. J. (2017). https://doi.org/10.15407/tpwj2016.12.04.

[38] B. Schmaling, A. Hartmaier, Determination of plastic material properties by analysis of residual imprint geometry of indentation, J. Mater. Res. 27 (2012) 2167–2177. https://doi.org/DOI: 10.1557/jmr.2012.212.

[39] B. Singh, P. Singhal, K.K. Saxena, R.K. Saxena, Influences of Latent Heat on Temperature Field, Weld Bead Dimensions and Melting Efficiency During Welding Simulation, Met. Mater. Int. 27 (2021) 2848–2866. https://doi.org/10.1007/s12540-020-00638-4.